

# Experimental observation of the mobility edge in a waveguide with correlated disorder

U. Kuhl<sup>1</sup>, F.M. Izrailev<sup>2</sup>, A. A. Krokhin<sup>2</sup>, and H.-J. Stöckmann<sup>1</sup>

<sup>1</sup> *Fachbereich Physik, Universität Marburg, Renthof 5, D-35032 Marburg, Germany*

<sup>2</sup> *Instituto de Física, Universidad Autónoma de Puebla, Apartado Postal J-48, Puebla, 72570 México*  
(May 19, 2018)

The tight-binding model with correlated disorder introduced by Izrailev and Krokhin [PRL **82**, 4062 (1999)] has been extended to the Kronig-Penney model. The results of the calculations have been compared with microwave transmission spectra through a single-mode waveguide with inserted correlated scatterers. All predicted bands and mobility edges have been found in the experiment, thus demonstrating that any wanted combination of transparent and non-transparent frequency intervals can be realized experimentally by introducing appropriate correlations between scatterers.

PACS numbers: 72.15.Rn, 72.20.Ee, 73.20.Jc

Starting from the pioneering paper by Anderson [1], a lot of progress has been achieved in the theoretical study of 1D tight-binding models. This model includes a wide range of different physical situations lying in between two limit cases: ideal periodic lattices where all states are extended, and completely random lattices where any state is exponentially localized. Specific interest has been paid to the so-called pseudo-random (or deterministic aperiodic) potentials which demonstrate either localization or delocalization, depending on their parameters [2–4]. A widely used model is described by the Harper equation with the site potential  $V_n = \epsilon \cos(2\pi\alpha n)$ . For  $\alpha$  irrational, the incommensurability of the potential gives rise to a localization-delocalization transition (for all states) when the amplitude  $\epsilon$  passes through the critical value  $\epsilon_{cr} = 2$ , see e.g., Ref. [5]. For fixed  $\epsilon$  the energy spectrum of the Harper equation exhibits the famous Hofstadter butterfly [6] when  $\alpha$  scans the interval  $[0, 1]$ . This rather exotic spectrum was recently observed experimentally [7] by making use of the equivalence of the Harper equation and the wave equation in a single-mode electromagnetic waveguide with point-like scatterers.

For a long time a coexistence of localized and extended states in the spectrum of eigenenergies of 1D random potentials was considered to be impossible. However, it was shown in Refs. [8,9] that a *discrete* set of delocalized states appears if short-range correlations are introduced in a random potential. This is done by repeating twice each value of site potential (dimer model). Recently discrete extended states have been observed in the experiment with GaAs-AlGaAs random superlattices [10].

A general case of 1D potential in tight-binding approximation with arbitrary correlations was considered in Ref. [11]. A direct relation between the pair correlation function and the localization length has been derived. This relation shows that the mobility edge does exist in 1D geometry. A few examples of potentials with correlated disorder were given. All these potentials necessarily contain the long-range correlations which thus give rise to a *continuum* set of delocalized states and to mobility edge.

In this Letter we exploit the analogy between the propagation of quantum particle and electromagnetic wave, in order to demonstrate experimentally the existence of the mobility edge in 1D geometry. The experimental set-up is shown in Fig. 1. It is the same as has been already used in the microwave realization of the Hofstadter butterfly [7]. From the top of a waveguide of total length of 2.15 m 100 micrometer screws can be turned in. By varying the lengths of the micrometer screws different scattering arrangements can be realized. Complete information about the scattering matrix of a given arrangement is obtained via two antennas at the ends of the waveguide using a Wiltron 360B network analyzer.

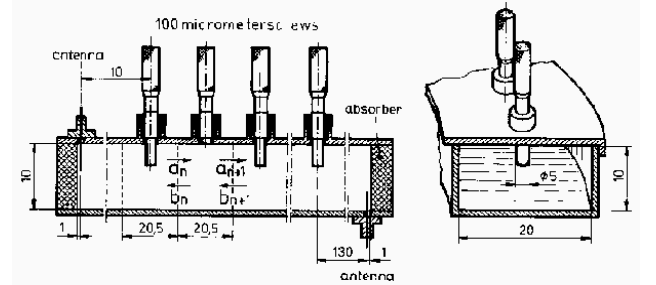


FIG. 1. Experimental set-up. All dimensions are given in mm.

If the screws are approximated by delta scatterers, the propagation of a single mode through the waveguide is described by the wave equation for the Kronig-Penney model,

$$\psi''(z) + E\psi(z) = \sum_{n=-\infty}^{\infty} EU_n\psi(z_n)\delta(z - nd). \quad (1)$$

Here the wave function  $\psi$  is associated with electric field of the  $TE$ -mode, and the energy is given by  $E = k^2$ , where  $k$  is the wavenumber. We write Eq. (1) in the discrete form [12],

$$\psi_{n+1} + \psi_{n-1} = [2 \cos(kd) + U_n kd \sin(kd)] \psi_n, \quad (2)$$

where  $\psi_n \equiv \psi(z_n)$ . The potential strength  $U_n = \epsilon + \epsilon_n$  is

split into two parts, its mean value  $\epsilon = \langle U_n \rangle$  and fluctuations  $\epsilon_n$ . Our treatment is based on the approach [13] which allows one to express the quantum model (1) in terms of the classical two-dimensional Hamiltonian map,

$$\begin{aligned} p_{n+1} &= (p_n + A_n x_n) \cos \mu - x_n \sin \mu, \\ x_{n+1} &= (p_n + A_n x_n) \sin \mu + x_n \cos \mu, \end{aligned} \quad (3)$$

where  $x_n = \psi_n$  is the position and  $p_n$  is the conjugate canonical momentum. This map describes the behavior of a linear oscillator subjected to linear periodic delta-kicks. The amplitude  $A_n$  of these kicks is defined as

$$A_n = \frac{k\epsilon_n \sin(kd)}{\sin \mu}, \quad (4)$$

and the phase shift  $\mu$  between two kicks is given by the dispersion relation for the Kronig-Penney model

$$2 \cos \mu = 2 \cos(kd) + kd\epsilon \sin(kd), \quad 0 \leq \mu \leq \pi. \quad (5)$$

The parameter  $\mu$  plays the role of the Bloch number and the width of the Bloch band is defined by  $\epsilon$ . In this approach localized quantum states correspond to trajectories which are unbounded in the classical phase space  $(p, x)$  when  $n \rightarrow \infty$ . Contrary, extended states are represented by bounded trajectories.

It is convenient to introduce the action-angle variables  $(r, \theta)$  according to the standard relations,  $x = r \sin \theta$ ,  $p = r \cos \theta$ . Then the inverse localization length can be defined as

$$l^{-1}(E) = \lim_{N \rightarrow \infty} \frac{1}{N} \sum_{n=1}^N \ln \left( \frac{r_{n+1}}{r_n} \right), \quad (6)$$

where

$$\frac{r_{n+1}}{r_n} = \sqrt{1 + A_n \sin(2\theta_n) + A_n^2 \sin^2 \theta_n}. \quad (7)$$

This definition coincides with the standard one  $l^{-1} = \langle \ln |\psi_{n+1}/\psi_n| \rangle$  [12] inside the allowed energy bands [14]. Here the brackets stand for the average over  $n$ .

This Hamiltonian map approach turns out to be very effective in the study of completely disordered potentials [14] as well as potentials with correlated disorder [11,13]. In particular, in Ref. [11] the expression for the localization length for the tight-binding model with *any* kind of correlations in the potential has been obtained. Since the relation (2) has the form of the tight-binding model, one can use the results of Ref. [11]. Then the inverse localization length for the Kronig-Penney model reads,

$$l^{-1}(E) = k^2 \frac{\langle \epsilon_n^2 \rangle \sin^2(kd)}{8 \sin^2 \mu} \varphi(\mu), \quad (8)$$

$$\varphi(\mu) = 1 + 2 \sum_{m=1}^{\infty} \xi_m \cos(2\mu m). \quad (9)$$

where  $\xi_m = \langle \epsilon_{n+m} \epsilon_n \rangle / \langle \epsilon_n^2 \rangle$  is the dimensionless binary correlator.

Relation (8) is a starting point to obtain the conditions under which the mobility edges exist for 1D random potentials. The function  $\varphi(\mu)$  in Eq. (9) is defined through its Fourier coefficients  $\xi_m$ . Then for a given dependence  $\varphi(\mu)$  the correlators can be calculated via

$$\xi_m = \frac{2}{\pi} \int_0^{\pi/2} \varphi(\mu) \cos(2m\mu) d\mu. \quad (10)$$

Now the problem is reduced to the construction of potentials having given correlators. Leaving mathematical details for a complete publication [15], we give here the final formula for set of random potentials with appropriate binary correlation function [16]:

$$\epsilon_n = \sqrt{\langle \epsilon_n^2 \rangle} \sum_{m=-\infty}^{+\infty} \beta_m Z_{n+m}, \quad (11)$$

$$\beta_m = \frac{2}{\pi} \int_0^{\pi/2} \sqrt{\varphi(\mu)} \cos(2m\mu) d\mu. \quad (12)$$

Here  $Z_n$  are random numbers with mean zero and variance one. It is easy to check that the dimensionless correlator of the site potential Eq. (11) coincides with the Fourier coefficient (10). Eqs. (8)-(12) give an explicit solution of the inverse problem, since they reconstruct random potentials from the dependence  $l(E)$ . The existence of the sharp mobility edges means that the function  $l^{-1}(E)$  has only finite (small) number  $\nu$  of derivatives at the corresponding energies. Then, the Fourier coefficients (10) decay slowly,  $\xi_m \sim m^{-(\nu+1)}$  for  $m \gg 1$ . This means that mobility edges are due to the *long-range correlations* in the random potential. Numerical data [11] for the step-function dependence ( $\nu = 0$ ) of  $\varphi(\mu)$  show that the localization length, indeed, reveals sharp mobility edges. Mobility edges obtained for self-affine potentials [17] are also due to the long-wavelength component of correlation function.

Let us now construct a random potential which results in the following function  $\varphi(\mu)$  (we chose this function to be symmetrical with respect to the point  $\mu = \pi/2$ ),

$$\varphi(\mu) = \begin{cases} C_0^2, & 0 < \mu_1 < \mu < \mu_2 < \pi/2 \\ 0, & \mu < \mu_1; \pi/2 > \mu > \mu_2. \end{cases} \quad (13)$$

Here  $C_0^2 = \pi/2(\mu_2 - \mu_1)$  is the normalization constant obtained from the condition  $\xi_0 = 1$ . This dependence exhibits four sharp ( $\nu = 0$ ) mobility edges in the first allowed zone. Their positions are given by two pairs of roots of Eq. (5) with  $\mu = \mu_1$  and  $\mu = \mu_2$ . Using Eq. (12) one obtains  $\beta_0 = 2C_0(\mu_2 - \mu_1)/\pi$  and

$$\beta_m = \frac{C_0}{\pi m} \{ \sin(2m\mu_2) - \sin(2m\mu_1) \}. \quad (14)$$

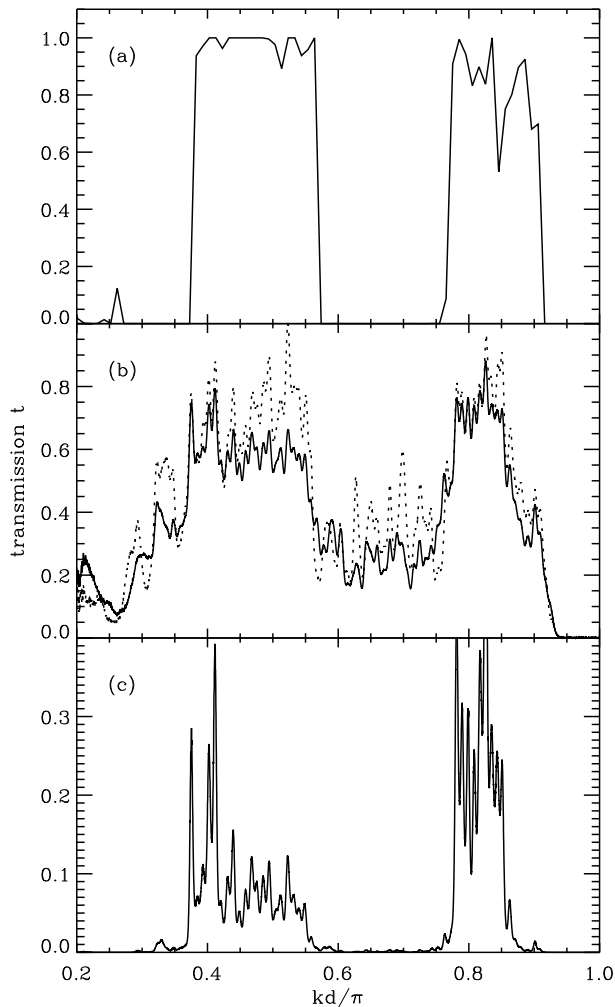


FIG. 2. Transmission through the 1D random sequence with correlation governed by Eq. (13): (a) numerical results for  $N = 10^4$  scatterers, (b) microwave transmission through an array of  $N = 100$  scatterers (dotted line) and average over five different measurements (solid line), (c) microwave transmission through an array of  $N = 500$  scatterers obtained by multiplying the transfer matrices of five individual measurements.

Experimentally it is difficult to measure the localization length directly. The accessible quantity is the transmission coefficient for a finite sample. Similar to the localization length, the transmission coefficient  $t_N$  can be expressed in terms of the classical map (3) [13],

$$t_N = \frac{4}{2 + r_{1N}^2 + r_{2N}^2}. \quad (15)$$

Here  $r_{1N}$  and  $r_{2N}$  are the radii of the trajectories at time  $N$ , starting at a radius  $r_0 = 1$  and angles  $\theta_0 = 0$  and  $\pi/2$ , respectively. This geometrical interpretation of the transmission coefficient is very useful for understanding its generic properties as well as for numerical simulations.

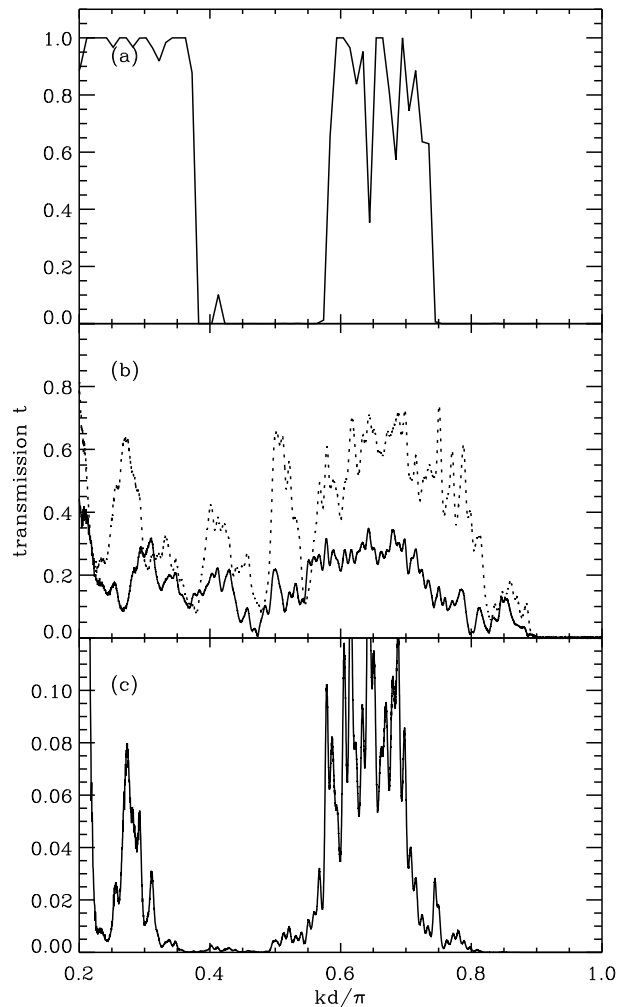


FIG. 3. Same as Fig. 2 but for the complementary potential, see in the text.

A sequence of scattering strengths  $\{\epsilon_n\}$  of the length  $N = 10^4$  was generated by calculating  $\beta_m$  from Eq. (14) with  $\mu_1/\pi = 0.2$  and  $\mu_2/\pi = 0.4$ , and substituting the result into Eq. (11). Fig. 2(a) shows the resulting transmission for  $\sqrt{\langle \epsilon_n^2 \rangle} = 0.1$  and  $\epsilon = -0.1$ . This value for  $\epsilon$  was obtained from Eq. (5) by adjusting the width of the allowed band to the experimental data. Experimental data are shown in Figs. 2(b,c). The mobility edges are clearly seen near the points  $kd/\pi = 0.38, 0.57, 0.76$  which are the roots of Eq. (5) with  $\mu/\pi = 0.4, 0.6, 0.8$  at the r.h.s. Transmission spectrum ends at the band edge,  $kd/\pi = 0.91$  for  $\mu = \pi$ . Data below  $kd/\pi = 0.2$  are not shown because of strong absorption in the waveguide at low frequencies.

We have also calculated and measured the transmission through the potential which is complementary to the previous one. Namely, it is transparent in the regions  $0.2 < \mu < 0.4$ ,  $0.6 < \mu < 0.8$  and untransparent otherwise. For this case coefficients  $\beta_m$  have opposite sign,  $\beta_0 = \frac{2C_0}{\pi}(\mu_1 - \mu_2 + \frac{\pi}{2})$ , and  $C_0^2 = \frac{\pi}{2(\mu_1 - \mu_2 + \pi/2)}$ . The

results are shown in Fig. 3(a) for the same parameters  $\epsilon_0$ ,  $\epsilon$ , and  $N$  as above. In this case again we got a reasonable agreement between analytical, numerical, and experimental data for the positions of the mobility edges.

For the experiment we used a segment of the length of  $N = 500$  from each of mutually complementary random sequences in order to create the appropriate scattering arrangements in the waveguide. The  $\epsilon_n$  were mapped into screw lengths by identifying the minimum  $\epsilon_n$  value with a length of 0 mm and the maximum value with a length of 3 mm. The average screw length of 1.5 mm determines the width of the Bloch bands [7]. This procedure ignores the phase shift due to the scatterers which probably is responsible for the negative value of  $\epsilon$  (see above). Five measurements were performed with each random sequence. In one measurement a transmission through a realization of hundred scatterers have been measured. The dotted lines in Fig. 2b and 3b show the results of a single measurement, the solid lines represent the results of averaging over all five measurements. The expected transmission pattern is already visible. But we can do even better. Since in each measurement the complete  $2 \times 2$  scattering matrix  $S_n (n = 1, \dots, 5)$  has been obtained, the corresponding transfer matrix  $T_n$  is available as well. Then the total transfer matrix  $T$  is the matrix product,  $T = \prod_{n=1}^5 T_n$ . Thus it is possible to study the transmission through arbitrary long sequences of scatterers with a set-up containing only 100 of them. However, because of absorption this technique is limited in our case to a total of about 1000 scatterers. Figs. 2c and 3c show such transmission spectra. In both cases the expected transparent and non-transparent regions are clearly reproduced.

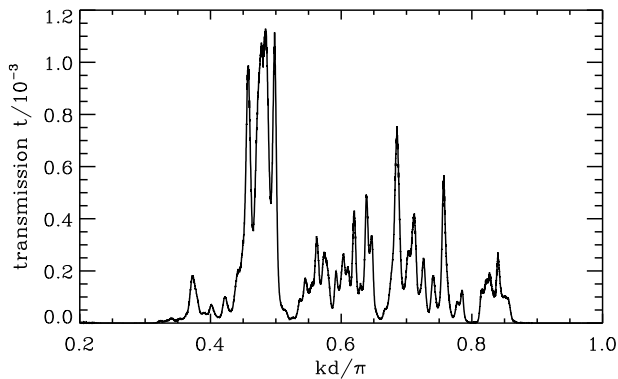


FIG. 4. Microwave transmission through a random arrangement of  $N = 500$  scatterers obtained by multiplying the transfer matrices of five individual measurements.

As a check we studied in addition the transmission through the uncorrelated random sequence of 500 scatterers. The result is shown in Fig. 4. Here the transmission is approximately 100 times smaller as for the sequences with correlated disorder within the transparent region.

Finally we would like to mention that Eq. (1) does not

take into account waveguide effects in the device. That is why one cannot expect a complete similarity in the behavior of the transmission coefficient obtained numerically with that measured in the experiment. Nevertheless, this equation allows one to calculate a correlated potential which being mapped to the length of scatterers, reproduces any prescribed structure of transparent and untransparent frequency zones. This direct mapping turns out to be rather successful if only the lowest mode of the waveguide is excited. For higher modes one might expect stronger influence of the waveguide effects.

The idea to this cooperation was developed during a workshop at the International Center for Sciences in Cuernavaca in November 1998. Final discussions took place during another workshop at the MPI for Complex Systems in Dresden in May 1999. We thank the organizers of the workshops for the invitations and the institutions for their hospitality which made this work possible. This work was supported by CONACyT (Mexico) Grants No. 26163-E and No. 28626-E and by the DFG via the Sonderforschungsbereich 185.

- 
- [1] P. Anderson, Phys. Rev. **109**, 1492 (1958).
  - [2] J. Bellisard, A. Formoso, R. Lima, and D. Testard, Phys. Rev. B **26**, 3024 (1982).
  - [3] M. Griniasty and S. Fishman, Phys. Rev. Lett. **60**, 1334 (1988).
  - [4] S. D. Sarma, S. He, and X. Xie, Phys. Rev. Lett. **61**, 2144 (1988).
  - [5] T. Geisel, R. Ketzmerick, and G. Petschel, in *Quantum Chaos*, edited by G. Casati and B. Chirikov (Cambridge University Press, 1995), p. 633.
  - [6] D. Hofstadter, Phys. Rev. B **14**, 2239 (1976).
  - [7] U. Kuhl and H.-J. Stöckmann, Phys. Rev. Lett. **80**, 3232 (1998).
  - [8] D. Dunlap, H.-L. Wu, and P. Phillips, Phys. Rev. Lett. **65**, 88 (1990).
  - [9] P. Phillips and H.-L. Wu, Science **252**, 1805 (1991).
  - [10] V. Bellani *et al.*, Phys. Rev. Lett. **82**, 2159 (1999).
  - [11] F.M. Izrailev and A. Krokhin, Phys. Rev. Lett. **82**, 4062 (1999).
  - [12] I.M. Lifshitz, S. Gredeskul, and L. Pastur, *Introduction to the Theory of Disordered Systems* (Wiley, NY, 1988).
  - [13] F.M. Izrailev, T. Kottos, and G. Tsironis, Phys. Rev. B **52**, 3274 (1995); T. Kottos, G. Tsironis, and F.M. Izrailev, J. Phys. Condens. Matter **9**, 1777 (1997).
  - [14] F.M. Izrailev, S. Ruffo, and L. Tessieri, J. Phys. A: Math. Gen. **31**, 5263 (1998).
  - [15] F.M. Izrailev and A. Krokhin, unpublished.
  - [16] We are thankful to V. Sokolov for the suggestion concerning this algorithm.
  - [17] F. A. de Moura and M. L. Lyra, Phys. Rev. Lett. **81**, 3735 (1998).